

# Magnetization switching utilizing the magnetic exchange interaction

R. Schmidt, A. Schwarz,<sup>\*</sup> and R. Wiesendanger*Institute of Applied Physics, University of Hamburg, Jungiusstrasse 11, 20355 Hamburg, Germany*

(Received 6 January 2012; revised manuscript received 27 September 2012; published 5 November 2012)

We demonstrate the feasibility of observing and inducing magnetization switching using the distance dependence of the magnetic exchange interaction. The experiments were performed employing an atomic force microscopy setup on the antiferromagnetic iron monolayer on the (001) surface of tungsten with magnetic tips that behaved like independent superparamagnetic clusters with uniaxial anisotropy. Applying the Néel-Brown law, we were able to determine energy barriers from lifetimes measured at different distances with and without external magnetic field. Our findings suggest that the distance dependence of the magnetic exchange interaction can be utilized to monitor and control magnetization dynamics on the atomic level.

DOI: [10.1103/PhysRevB.86.174402](https://doi.org/10.1103/PhysRevB.86.174402)

PACS number(s): 75.75.-c, 68.37.Ps, 75.30.Et

## I. INTRODUCTION

Changing an external magnetic field is the most obvious way to control the magnetization direction of a specimen. In magnetic hard discs this method has been in use for decades for data recording.<sup>1</sup> Similarly, the magnetization direction of magnetic nanodots can be switched with the help of the local stray field emanating from a ferromagnetic tip in a magnetic force microscopy (MFM) setup.<sup>2</sup> The opposite, i.e., switching of the tip magnetization direction, has been observed as well.<sup>3</sup> More recently, spin transfer torque has been established to switch the magnetization direction of a free magnetic layer with respect to a fixed magnetic layer by a spin-polarized tunneling current in a planar spin-valve or magnetic tunnel junction geometry.<sup>4,5</sup> On an even smaller length scale it has been demonstrated that the spin-polarized tunneling current across a vacuum gap in a spin-polarized scanning tunneling microscopy (SP-STM) setup, can be employed to selectively reverse the magnetization direction of individual magnetic nanoislands.<sup>6</sup> Here, we also use a local probe technique in a tip-sample geometry, but instead of a spin-polarized tunneling current, as in SP-STM, or a long-range magnetostatic stray field, as in MFM, we utilize the distance dependence of the short-range magnetic exchange interaction utilizing magnetic exchange force microscopy (MExFM).

MExFM, an atomic force microscopy (AFM) variant, opened up the possibility of atomic-scale studies with single-spin sensitivity.<sup>7,8</sup> Its spectroscopic mode, i.e., magnetic exchange force spectroscopy (MExFS), permits directly measuring magnitude and distance dependence of the magnetic exchange interaction quantitatively.<sup>9</sup> In this study we apply both methods to control the switching probability of a superparamagnetic cluster with uniaxial anisotropy via the distance dependence of the magnetic exchange interaction. By measuring lifetimes, we could determine the energy barrier between both possible states and study the influence of an externally applied magnetic field. In the present investigation it is the tip apex that exhibits properties of a superparamagnetic cluster. However, we envisage that MExFM and MExFS are appropriate tools to characterize magnetization dynamics of small magnetic particles or even atoms that are prepared in a more controlled fashion on substrates similar to previous investigations performed with SP-STM. Note that the advantage of a force-based technique

compared to a tunneling current based detection scheme in this context is that spin torque and joule heating effects are absent and it can be applied to nonconducting sample systems.

## II. EXPERIMENTAL METHODS

As the surface we chose the Fe monolayer on W(001), which exhibits an antiferromagnetic spin structure with out-of-plane anisotropy.<sup>10</sup> A magnetically sensitive tip can be straightforwardly identified by imaging the  $c(2 \times 2)$  antiferromagnetic unit cell with atomic resolution.<sup>8</sup> Such tips were prepared by depositing a few-nanometer Cr onto Si tips covered by a native oxide layer. Since collisions with the surface were frequently provoked to prepare a suitable tip, material transfer usually leads to an Fe terminated tip apex. Data acquisition was performed with our homebuilt AFM setup (Hamburg design), which is equipped with a 5 T superconducting magnet and operated at 8.1 K in ultrahigh vacuum.<sup>11</sup> For imaging in the noncontact regime, the frequency modulation technique was employed.<sup>12</sup> All data were obtained with constant oscillation amplitude  $A$ . MExFM images were recorded at a constant frequency shift  $\Delta f$ . In the spectroscopy mode (MExFS) at every  $(x, y)$  image point a  $\Delta f(z)$  curve was recorded as well. This technique is known as three-dimensional force field spectroscopy (3D-FFS).<sup>13</sup> During imaging and while recording distance-dependent data the dissipation  $E_D$ , i.e., the energy required to keep  $A$  constant, was recorded as well, which allows us to distinguish between structurally stable and unstable tip apices.<sup>9</sup>

## III. EXPERIMENTAL OBSERVATION OF MAGNETIZATION SWITCHING EVENTS

Figure 1(a) shows an image scanned from bottom to top with a magnetically sensitive tip. The overlaid grid shows the position of Fe atoms, i.e., the  $p(1 \times 1)$  chemical surface unit cell. Since only every second Fe atom is imaged as maximum, the image contrast represents the antiferromagnetic  $c(2 \times 2)$  spin structure (see dashed square). In the surface area marked by the frame, a switching event occurred (see inset), whereby the minima appear as maxima and vice versa. The scan line with the switching event is displayed together with a sketch that explains the contrast reversal [cf. Figs. 1(b) and 1(c)]. Note

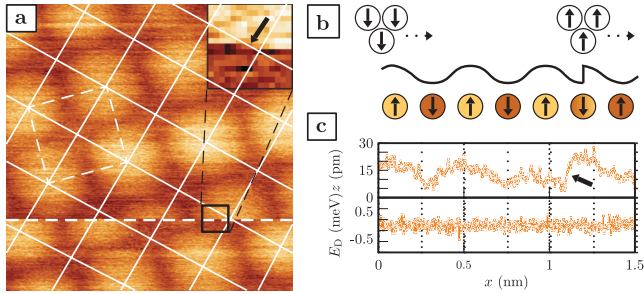


FIG. 1. (Color) (a) The  $(1.5 \times 1.5) \text{ nm}^2$  MExFM image of the Fe monolayer on W(001) scanned from bottom to top. The grid marks the position of Fe atoms. Minima and maxima correspond to surface atoms with magnetic moments aligned parallel (P site) and antiparallel (AP site) to the spins at the tip apex, respectively. The dashed square represents the antiferromagnetic  $c(2 \times 2)$  unit cell. On the dashed line within the marked area (see inset) the switching event took place, resulting in a contrast reversal. Parameters are  $\Delta f = -5.8 \text{ Hz}$ ,  $c_z = 143 \text{ N/m}$ ,  $A = 2.81 \text{ nm}$ ,  $f_0 = 185 \text{ kHz}$ ,  $B = 4.5 \text{ T}$ ,  $Q = 62835$ . (b) Sketch of the contrast reversal after switching of the magnetization direction at the tip apex. (c) Actual scan line on which the switching occurred. The featureless dissipation signal indicates a pure magnetic switching without structural reconfigurations at the tip apex.

that the spins at the tip apex are reversed and this reversal is detected via their interaction with the unchanged surface spins. From the featureless dissipation signal in Fig. 1(c) and the absence of any  $z$  offset due to a tip that becomes either longer or shorter and since the registry between the overlaid grid and positions of maxima and minima, respectively, remains perfect after the switching event, we can infer that the magnetization reversal is not accompanied by any structural change at the tip apex.<sup>14</sup>

According to theoretical calculations, maxima and minima in MExFM images denote Fe atoms aligned antiparallel (AP site) and parallel (P site) with respect to the tip magnetic moment, respectively.<sup>8</sup> Note that this assignment is true for Cr as well as for Fe terminated tips. Thus, in Fig. 1(a) the tip expectedly switches from a P to the energetically preferred AP configuration (the switching occurs on a minimum, which becomes a maximum). The transition is not as sharp as sketched in Fig. 1(b) but takes about 5 ms (5 data points). However, this is not the real switching time, which is several orders of magnitude faster, but is related to the much slower response time of the  $z$  feedback during data acquisition. Since the magnetic corrugations before and after the switching event are identical ( $\approx 14 \text{ pm}$ ), we can infer that the magnetization direction of the tip rotated by  $180^\circ$ . Note that the line of arguments is still correct if the spins in the tip and sample are not exactly collinear. In this case one just has to consider the projection of the magnetization direction in the tip apex on the surface normal.

The data displayed in Fig. 2 stem from a tip which exhibits frequent contrast reversals during imaging. With this tip a complete 3D-FFS data set was recorded concurrently with the image data displayed in the inset. The slanting of the topography image is related to piezo creep while recording the 3D-FFS data over 7 h. Nevertheless, the magnetic contrast as well as the reversal events can be clearly identified. These data

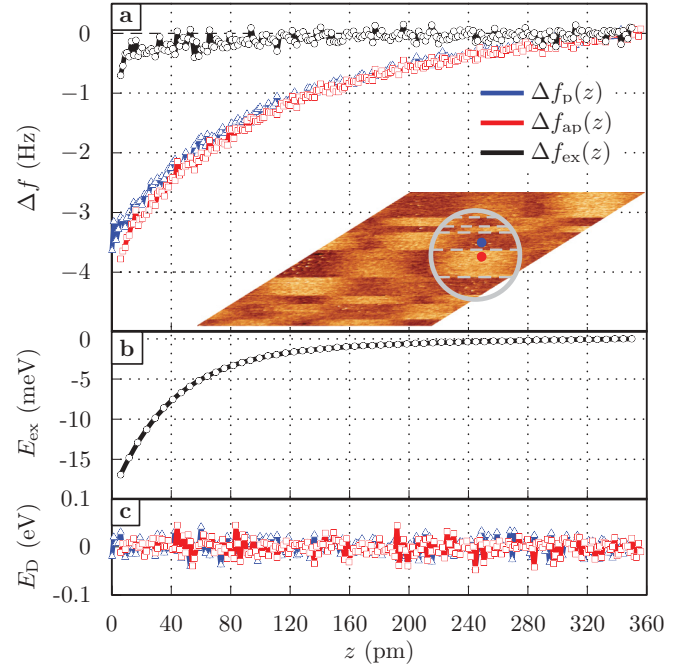


FIG. 2. (Color) Distance dependence of the magnetic exchange interaction  $E_{\text{ex}}$  and the energy dissipation  $E_{\text{D}}$  measured for a tip that frequently reversed its magnetization direction (see inset). (a) The two displayed  $\Delta f(z)$  curves stem from a complete 3D-FFS data set and were recorded approximately on the center of the same encircled Fe atom, but with the tip apex spins aligned parallel (P, blue) and antiparallel (AP, red) relative to the spin of the surface Fe atom, respectively. The difference  $\Delta f_{\text{ex}}(z) = \Delta f_{\text{AP}}(z) - \Delta f_{\text{P}}(z)$  (black line) was used to calculate  $E_{\text{ex}}(z)$  in (b). The simultaneously recorded featureless  $E_{\text{D}}(z)$  curve in (c) is characteristic of a structurally stable tip.<sup>9</sup> Parameters are  $\Delta f = -5.6 \text{ Hz}$ ,  $c_z = 145.5 \text{ N/m}$ ,  $A = 3.83 \text{ nm}$ ,  $f_0 = 187 \text{ kHz}$ ,  $B = 5 \text{ T}$ ,  $Q = 318000$ .

enable us to quantify the magnitude and distance dependence of the magnetic exchange interaction  $E_{\text{ex}}(z)$  and the energy dissipation  $E_{\text{D}}(z)$ , using a procedure presented in Ref. 9: The red and blue dots mark the positions where the two  $\Delta f(z)$  curves shown in Fig. 2(a) were taken. The two selected curves were acquired approximately above the center on the same Fe atom, where the exchange interaction is largest, but with oppositely oriented spins at the tip apex. Therefore, blue and red curves represent the tip apex in P and AP configurations, respectively. Indicated by the constant and featureless dissipation signals shown in Fig. 2(c) for both configurations, the atomic configuration at the tip apex was the same for both curves at every tip sample distance (cf. Ref. 9). This interpretation is also supported by the even characteristic of both  $\Delta f(z)$  curves as they are indistinguishable at large separations and smoothly split into two branches at smaller separations, where the magnetic exchange interaction becomes significant. After subtracting both curves the magnetic exchange energy  $E_{\text{ex}}$  [Fig. 2(b)] can be calculated from the resulting  $\Delta f_{\text{ex}}(z)$  curve [black curve in Fig. 2(a); see Ref. 9 for details]. The  $E_{\text{ex}}(z)$  relationship reflects how much the AP configuration between tip and sample spins is favored compared to the P configuration and how this energy difference depends on the tip-sample distance. For this tip  $E_{\text{ex}}$  is about  $-16.9 \text{ meV}$  at

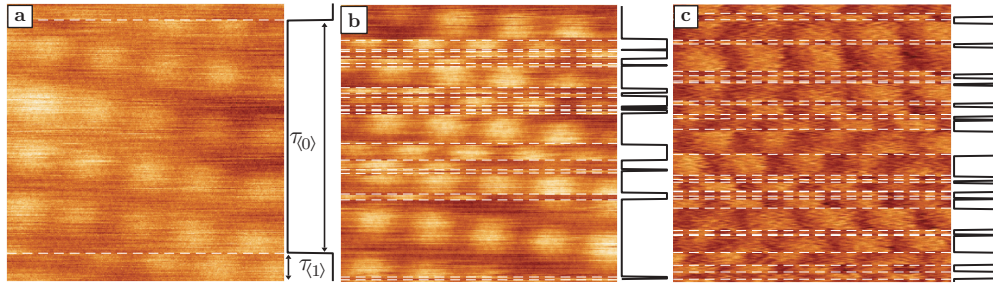


FIG. 3. (Color online) (a)–(c) The  $(2 \times 2) \text{ nm}^2$  MEXFM images demonstrating the distance and magnetic field dependence of the switching. (a) and (b) were recorded in  $B = 4.5 \text{ T}$  with the same tip, but in (b) the tip was  $40 \text{ pm}$  closer to the surface. Clearly, the number of switching events increased drastically. The two lifetimes,  $\tau_{(0)}$  and  $\tau_{(1)}$ , are unequal. (c) was recorded with another tip and in  $B = 0 \text{ T}$ . Lifetimes  $\tau_{(0)}$  and  $\tau_{(1)}$  are also unequal, but the difference is significantly smaller than in (b) with  $B \neq 0$ .

the smallest separation, where the image data visible in the inset were recorded and where the tip frequently reversed its magnetization direction. Note that the absolute  $z$  scale cannot be determined experimentally. However, comparison with theoretical calculations presented in Ref. 9 suggest a real tip-sample distance of about  $400 \text{ pm}$  at the smallest separation, i.e., at  $z = 0$  in Fig. 2.

Figure 3 summarizes our experimental findings regarding the distance and magnetic field dependence of the switching behavior. In all three images the tips do not exhibit site- or spin-dependent dissipation and can thus be regarded as structurally stable. The corresponding tip states, denoted as  $\langle 0 \rangle$  and  $\langle 1 \rangle$ , respectively, are plotted to the right. Since the scan speed is known, the duration, in which the tip state remains unchanged, i.e., its lifetime, can be determined. Figures 3(a) and 3(b) were acquired with the same tip in an external flux density  $B = 4.5 \text{ T}$  applied perpendicular to the sample, but at different  $\Delta f$  set points, i.e.,  $-25$  and  $-29 \text{ Hz}$ , respectively, as Fig. 2(b) was recorded at a  $40\text{-pm}$  smaller tip-sample separation. According to Fig. 2(b) the corresponding increase of the magnetic exchange interaction at small tip-sample separations can be roughly estimated to be about  $10 \text{ meV}$ . The

strong increase of the number of switching events from 2 to 22 demonstrates that the switching probability can be influenced via the tip-surface separation. For the relatively large number of switching events in Figs. 3(b) and 3(c), the mean lifetimes  $\tau_{(0)}$  and  $\tau_{(1)}$  can be determined [for Fig. 3(a) no reasonable analysis is possible]. For Fig. 3(b) we find different lifetimes, i.e.,  $\tau_{(0)} = (45 \pm 17) \text{ s}$  and  $\tau_{(1)} = (15 \pm 4) \text{ s}$ , respectively. Figure 3(c), which has been recorded with another tip and in zero field, also exhibits different lifetimes, but with  $\tau_{(0)} = (27 \pm 5) \text{ s}$  significantly closer to  $\tau_{(1)} = (17 \pm 3) \text{ s}$  than for  $B = 4.5 \text{ T}$ . As in Fig. 1, all switching events in Fig. 3 were initiated on a minimum, which then became a maximum, meaning that the tip magnetization always changed from a P into an AP configuration.

#### IV. NÉEL-BROWN MODEL INCLUDING MAGNETIC EXCHANGE INTERACTION

For the following discussion we tentatively assume that a nanotip at the apex of the macroscopic tip pyramid exists that behaves like a superparamagnetic cluster with uniaxial anisotropy and can switch its magnetization direction across

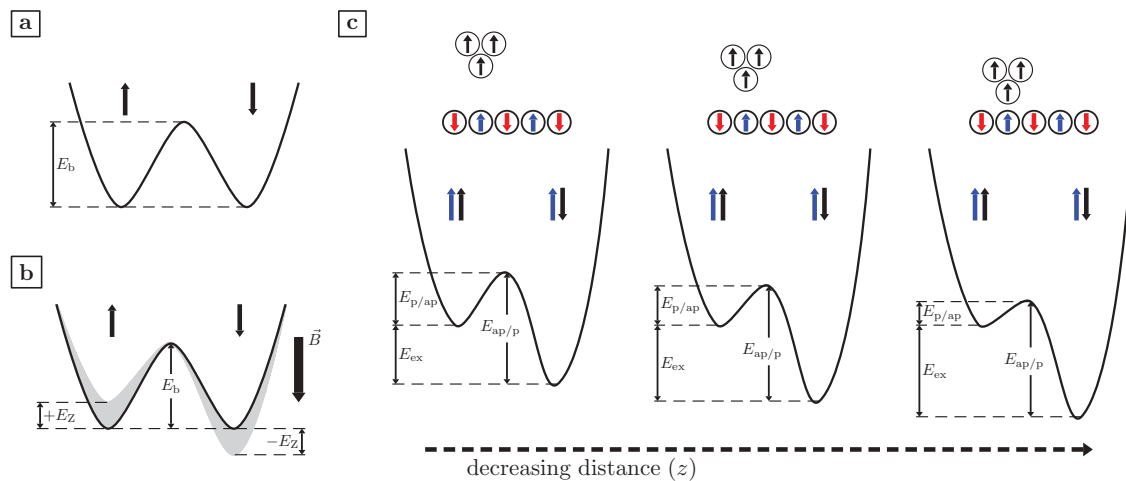


FIG. 4. (Color online) (a) depicts the two states of a magnetic particle with uniaxial anisotropy without external magnetic field. In (b) the shaded area represents the relative shift of the two states due to the Zeeman energy in an external magnetic field. (c) shows the influence of the distance-dependent magnetic exchange energy between tip and surface on the two states. The decreased barrier height between the P and AP configurations explains the experimentally observed increased switching rate after decreasing the tip-sample separation [cf. Figs. 3(a) and 3(b)].

an energy barrier via thermal excitation. The general behavior of such a superparamagnetic cluster is depicted in Figs. 4(a) and 4(b): In zero field the two states of magnetization are separated by a single symmetric barrier  $E_b$ . According to the Néel-Brown law  $\tau = 1/\nu_0[\exp(-E_b/k_B T)]$  (Refs. 15,16) the lifetime  $\tau$  depends on the relation between  $E_b$  and thermal energy  $k_B T$ , as well as, although to a much lesser degree, on the attempt frequency  $\nu_0$ . In the presence of an external magnetic field  $B$  the energy minimum for the magnetization direction parallel (antiparallel) to  $B$  is lowered (elevated) by the Zeeman energy  $E_Z$ . As a result, the energy barrier becomes asymmetric, and the lifetimes of the magnetization state parallel to  $B$  are different, i.e., larger, than the magnetization state antiparallel to  $B$ .

In the presence of a magnetic exchange force, the model has to be modified. Figure 4(c) explains the increased switching rate visible in the image data in Figs. 3(a) and 3(b). Treating the tip apex as a superparamagnetic cluster, its magnetization direction, and thus the spin of the foremost tip apex atom, can either point upwards or downwards (black arrows in the sketch). In whatever direction the spin at the tip apex actually points, during scanning it periodically changes its relative orientation with respect to the antiferromagnetic surface from AP to P configuration. As mentioned above, the AP configuration is energetically favored. Therefore, the energy barrier  $E_b$  becomes asymmetric at close tip-sample separations. The difference between the energy barriers from AP to P configuration and vice versa, i.e.,  $E_{AP/P}$  and  $E_{P/AP}$ , respectively, is the magnetic exchange energy  $E_{ex}$ . This immediately explains why switching events during topography imaging are initiated on minima, which represent P configurations between tip and sample spin. Note there is a different effect of the Zeeman energy due to an external magnetic field and the exchange energy: the former does affect both states symmetrically [cf. Fig. 4(a)], while the exchange energy does not. Since  $E_{ex}$  is distance dependent and increases at smaller separations (cf. Fig. 2), it is obvious that the difference between  $E_{P/AP}$  and  $E_{AP/P}$  is distance dependent as well and thus becomes larger for smaller tip-sample distances. Additionally, the increased

switching rate demonstrates that the energy barrier  $E_{P/AP}$  is actually lowered, as sketched in Fig. 4(c).

To understand the two different lifetimes found in Fig. 3(b) the presence of the magnetic exchange interaction plus an external magnetic field has to be considered. All four possible initial configurations between tip apex and sample spins are shown in Fig. 5. Since the corresponding energy barriers are all different, four different lifetimes exist. However, only two lifetimes (and not four) are observed because only transitions from the P to the AP configuration actually occur (leftmost and rightmost sketches in Fig. 5) because the energy barrier in the opposite direction is larger by the magnetic exchange energy  $E_{ex}$ . Thus, both lifetimes  $\tau_{(0)}$  and  $\tau_{(1)}$  correspond to transitions from the P into the AP configuration, but for the longer one, i.e.,  $\tau_{(0)}$ , the tip apex magnetization is parallel to the external magnetic field. Note that  $E_{ex}$  is much larger than  $E_Z$  because, according to Fig. 2 and Ref. 9, the former is on the order of 10 meV per atom, while the Zeeman energy for  $B = 5$  T for Fe is about 0.1 meV per atom.

Since the image displayed in Fig. 3(c) was recorded in zero field, the lifetimes for states  $\langle 0 \rangle$  and  $\langle 1 \rangle$  should be equal. As before, they both correspond to transitions from the P into the AP configuration, but now no magnetization direction at the tip apex is preferred. Indeed, the difference between both lifetimes is smaller, but still significant. We could imagine two possible explanations for this observation. First, the self-stray field emanating from the thin-film surface covering the whole macroscopic tip pyramid can act in the same way on the tip apex as an external magnetic field. Note that due to uncompensated spins at surfaces even an antiferromagnetic Cr coating can exhibit a small self-stray field. Second, a zero-field anisotropy could be induced by the geometric structure at the tip apex (it certainly will not possess spherical symmetry), which affects the local magnetocrystalline anisotropy energy.<sup>17</sup>

Applying the Néel-Brown law stated above, the energy barrier  $E_b = E_{P/AP}$  can be estimated. For the attempt frequency  $\nu_0$  we use the Larmor frequency, which is on the order of 1 GHz for Cr and Fe. The available thermal energy  $k_B T$  ( $T = 8.1$  K)

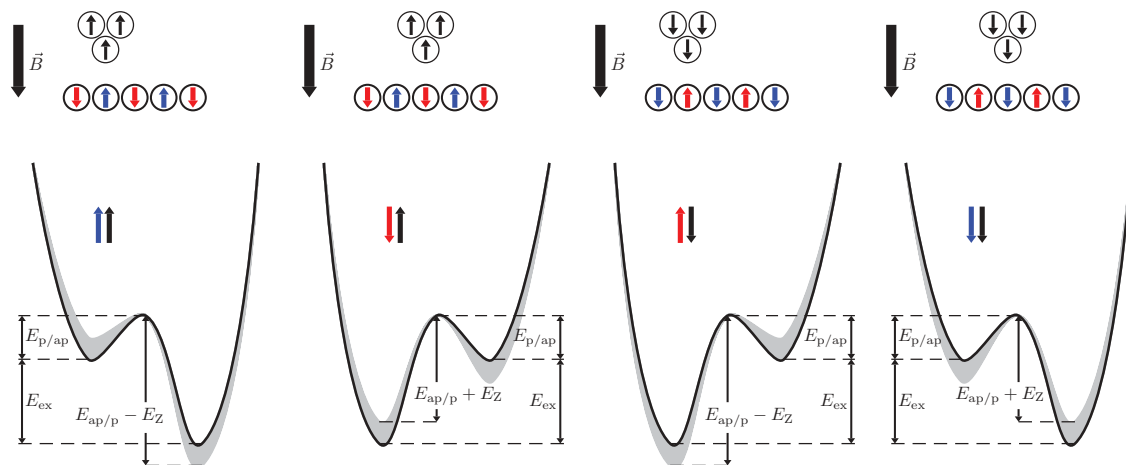


FIG. 5. (Color online) Combined effect of an external magnetic field and the magnetic exchange energy between the tip and sample on the energy landscape. Note that the magnetic exchange energy is much larger than the Zeeman energy. Since the AP configuration is energetically favored, only P to AP switching events are observed. Due to the Zeeman energy, the state with the tip apex magnetization parallel to the external magnetic field is preferred.

is about 0.7 meV. For Fig. 3(b) ( $B = 4.5$  T) the corresponding barrier heights  $E_{P/AP}$  are 16.3 meV ( $\tau_{(0)}$ ) and 17.1 meV ( $\tau_{(1)}$ ), respectively. The larger lifetime (higher-energy barrier) can be assigned to a tip apex with a magnetization direction parallel to the magnetic field. The difference of 0.8 meV ( $E_Z = \pm 0.4$  meV) corresponds to an effective Zeeman energy  $E_Z$  felt by the tip apex. In zero field [cf. Fig. 3(c)], the corresponding energy barriers are 16.4 meV ( $\tau_{(0)}$ ) and 16.8 meV ( $\tau_{(1)}$ ), respectively. In this case the difference of 0.4 meV could be attributed to a residual self-stray field from the Cr-covered tip due to uncompensated spins, as mentioned above. Note that different tips were used; hence the exact magnitude of the self-stray field in Figs. 3(b) and 3(c) can be different. Since  $E_{AP/P} = E_{P/AP} + E_{ex}$  and  $E_{ex}$  is on the order of 10 meV (estimated from Fig. 2), the corresponding lifetime is on the order of 1 year for  $E_{AP/P} = 26.4$  meV at 8.1 K, which justifies the presumption that all switching events are P to AP reversals.

We can also estimate energy barriers required for long-term stable imaging, e.g., no switching event over 24 h, or energy barriers, which result in too fast and thus nondetectable switching. At 8.1 K an energy barrier larger than 22 meV would lead to less than one switching event per day. Note that for experiments at room temperature the energy barrier has to be larger. Assuming a time resolution of 1 ms for MExFM, barrier heights below 10 meV would actually lead to an image contrast as if the tip were nonmagnetic.

Moreover, our experimental data allow us to roughly estimate the number of atoms in the nanotip that participate in the magnetization switching (it is certainly not the whole magnetic layer on the macroscopic tip that switches). The magnitude of the Zeeman energy of  $E_Z = \pm 0.4$  meV indicates that the nanotip in Fig. 3(b) consists of a few atoms only because, as already mentioned above, at 5 T the Zeeman energy is on the order of 0.1 meV per Fe atom. Another estimation is possible via the barrier height, which is determined by the magnetocrystalline anisotropy energy (MAE). Compared to typical values found in bulk samples, the MAE per atom is significantly larger on surfaces as well as within small clusters, i.e., typically on the order of 1 meV per atom or more.<sup>18</sup> Thus, an energy barrier of about 17 meV would indicate a nanotip made of 10–20 atoms.

It turns out that our tentative nanotip model is qualitatively and quantitatively consistent with our experimental observations. Indeed, the formation of nanotips on top of macroscopic tip pyramids is commonly assumed to explain atomic resolution imaging in atomic force microscopy.<sup>19,20</sup> However, it is not obvious how such a nanotip can be

magnetically independent from the rest of the tip, a prerequisite to observe paramagnetic behavior. We believe that the nanotip is actually not fully decoupled and that the remaining magnetic coupling to the rest of the tip is, in fact, responsible for the energy barrier. As mentioned in the experimental methods paragraph (Sec. II), magnetically sensitive tips are typically created by intended collisions between the tip and surface. Therefore, most likely, Fe from the surface was picked up, forming a nanotip. Such an Fe nanotip (magnetic cluster) could be only weakly coupled to the rest of the tip because the tip apex is strongly curved, and therefore atoms are not as well ordered as on a flat surface.<sup>21</sup> This situation would correspond to a grain boundary in polycrystalline materials, which are known to reduce magnetic exchange coupling.<sup>22</sup> The energy barrier between the two states of the nanotip would then stem from the residual magnetic coupling between the nanotip and Cr film. Additionally, the geometry of the nanotip could contribute to the energy barrier as well. Such a geometry-dependent energy barrier has been, in fact, found for small magnetic clusters.<sup>17</sup>

## V. SUMMARY AND CONCLUSIONS

In summary, the observation of the superparamagnetic behavior of such a tip during scanning of an antiferromagnetic surface with atomic resolution shows that MExFM and MExFS can be applied to study magnetization reversal processes with atomic resolution. Most interestingly, we demonstrated that the distance dependence of the magnetic exchange interaction can be measured and subsequently utilized to modify the energy barrier between two magnetic states in a controllable fashion. Future systematic studies can be envisaged to investigate the magnetization dynamics on small islands, molecules, or even single atoms. Moreover, with this force-microscopy-based scanning-probe method such sample systems can be prepared and studied on insulating substrates. It is noteworthy that the magnetic exchange force can also become relevant in STM studies, e.g., if conductance measurements through a single adatom on a surface are performed with a magnetic tip in the contact or near-contact regime.<sup>23</sup>

## ACKNOWLEDGMENTS

The authors thank S. Heinze, C. Lazo, S. Krause, and E. Vedmedenko for fruitful discussions. Financial support from the DFG (SFB 668-A5), from the ERC Advanced Grant FURORE, and from the Cluster of Excellence NANOSPIN-TRONICS is gratefully acknowledged.

\*Corresponding author. aschwarz@physnet.uni-hamburg.de

<sup>1</sup>D. A. Thompson and J. S. Best, *IBM J. Res. Dev.* **44**, 311 (2000).

<sup>2</sup>G. A. Gibson and S. Schultz, *J. Appl. Phys.* **73**, 4516 (1993).

<sup>3</sup>P. Grütter, D. Rugar, H. J. Mamin, G. Castillo, C. J. Lin, I. R. McFadyen, R. M. Valletta, O. Wolter, T. Bayer, and J. Greschner, *J. Appl. Phys.* **69**, 5883 (1991).

<sup>4</sup>D. C. Ralph and M. D. Stiles, *J. Magn. Magn. Mater.* **320**, 1190 (2008).

<sup>5</sup>G. A. Prinz, *Science* **282**, 1660 (1998).

<sup>6</sup>S. Krause, L. Berbil-Bautista, G. Herzog, M. Bode, and R. Wiesendanger, *Science* **317**, 1537 (2007).

<sup>7</sup>U. Kaiser, A. Schwarz, and R. Wiesendanger, *Nature (London)* **446**, 522 (2007).

<sup>8</sup>R. Schmidt, C. Lazo, H. Hölscher, U. H. Pi, V. Caciuc, A. Schwarz, R. Wiesendanger, and S. Heinze, *Nano Lett.* **9**, 200 (2009).

- <sup>9</sup>R. Schmidt, C. Lazo, U. Kaiser, A. Schwarz, S. Heinze, and R. Wiesendanger, *Phys. Rev. Lett.* **106**, 257202 (2011).
- <sup>10</sup>A. Kubetzka, P. Ferriani, M. Bode, S. Heinze, G. Bihlmayer, K. von Bergmann, O. Pietzsch, S. Blügel, and R. Wiesendanger, *Phys. Rev. Lett.* **94**, 087204 (2005).
- <sup>11</sup>M. Liebmann, A. Schwarz, S. M. Langkat, and R. Wiesendanger, *Rev. Sci. Instrum.* **73**, 3508 (2002).
- <sup>12</sup>T. R. Albrecht, P. Grütter, D. Horne, and D. Rugar, *J. Appl. Phys.* **69**, 668 (1991).
- <sup>13</sup>H. Hölscher, S. M. Langkat, A. Schwarz, and R. Wiesendanger, *Appl. Phys. Lett.* **81**, 4428 (2002).
- <sup>14</sup>Simultaneous structural and magnetic switching events at the tip apex do occur and can be identified [cf. Ref. 9]. Such tips are not considered in this paper because data recorded with them cannot be evaluated quantitatively with the simple model proposed here. However, we plan to discuss the general behavior of such tips in a more qualitative fashion in a separate publication.
- <sup>15</sup>L. Néel, *Ann. Geophys.* **5**, 99 (1949).
- <sup>16</sup>W. F. Brown, *Phys. Rev.* **130**, 1677 (1963).
- <sup>17</sup>G. M. Pastor, J. Dorantes-Davila, S. Pick, and H. Dreyssé, *Phys. Rev. Lett.* **75**, 326 (1995).
- <sup>18</sup>G. Bihlmayer, in *Reduced Dimensions II: Magnetic Anisotropy*, edited by S. Blügel (Forschungszentrum Jülich, Germany, 2005), p. C2.14.
- <sup>19</sup>M. Guggisberg, M. Bammerlin, C. Loppacher, O. Pfeiffer, A. Abdurixit, V. Barwich, R. Bennowitz, A. Baratoff, E. Meyer, and H. J. Güntherodt, *Phys. Rev. B* **61**, 11151 (2000).
- <sup>20</sup>A. S. Foster, C. Barth, A. L. Shluger, and M. Reichling, *Phys. Rev. Lett.* **86**, 2373 (2001).
- <sup>21</sup>In fact, most nanotips are so strongly coupled to the rest of the tip that they never switch (about 80% of our tips).
- <sup>22</sup>R. Fischer and H. Kronmüller, *J. Magn. Magn. Mater.* **184**, 166 (1998).
- <sup>23</sup>J. Bork, Y. Zhang, L. Diekhöner, L. Borda, P. Simon, J. Kroha, P. Wahl, and K. Kern, *Nat. Phys.* **7**, 901 (2011).